2025 European Conference on Computing in Construction

CIB W78 Conference on IT in Construction

Porto, Portugal
July 14-17, 2025

EVALUATION OF DIFFERENT UWB TAG PLACEMENTS ON CONSTRUCTION WORKERS FOR ENHANCING SAFETY

Umutcan Kılıç[1], Semra Çomu[1], and F. Serhan Daniş[2,3]
[1]Boğaziçi University, Türkiye
[2]Galatasaray University, Türkiye
[3]Université Gustave Eiffel, France

Abstract

Ultra-wideband (UWB) technology, offering high precision and low latency, emerges as a solution for accurate worker tracking to improve construction safety. However, non-line of sight (NLOS) conditions can impact its reliability. This study evaluates UWB tag placements on different body parts in a controlled walking experiment. Data from six participants were analyzed using t-Tests for accuracy and F-tests for consistency across different axes. Results show that head-mounted tags provide the highest accuracy, while tags attached around shoulders, waist, and knees deviate due to body shadowing. Findings emphasize the importance of optimal sensor placement for real-time worker tracking in construction.

Introduction

Construction projects are inherently high-risk environments due to their dynamic and complex nature. For instance, construction is the industry with the highest rate of fatal and non-fatal accidents, accounting for 22.9% of all fatal accidents and 12.2% of all non-fatal accidents in Europe (Eurostat, 2024). Construction workers face a number of different hazards on a daily basis, including falling from height, equipment-related accidents, and exposure to harmful substances, and the high frequency of occurrence of these hazards makes safety a critical component of the construction management domain. However, despite the increasing number of research studies on construction occupational safety management over the last decade, the still high rates of accidents raise questions about the effectiveness of the existing construction site safety practices (Newaz et al., 2022). As a result, many researchers shifted their focus to the implementation of advanced technologies in construction projects, such as 4D Computer-Aided Design (4D CAD), Building Information Modelling (BIM), Geographic Information Systems (GIS), laser scanning, online databases, photogrammetry, robotics and automation, sensor-based technologies, Unmanned Aerial Vehicles (UAVs), and Virtual Reality (VR), to overcome the shortcomings of existing practices in construction site health and safety (Akinlolu et al., 2020).

One important aspect of improving safety lies in understanding and managing the location of workers and equipment in real-time. For instance, various research focused on using Real Time Location Systems (RTLS) for improving construction safety and identified that RTLS offers potential improvements in terms of safety monitoring, accident prevention, behavior-based safety, safety alerts and warnings, ergonomics analysis and physiological status monitoring, communication-based safety, and on-site safety training (Soltanmohammadlou et al., 2019). Various RTLS have been developed to address the need for precise worker tracking in construction, including systems utilizing Computer Vision, Ultra-wide Band (UWB), Radio Frequency Identification (RFID), Bluetooth, Global Positioning System (GPS), and UAV technologies (Asadzadeh et al., 2020).

Computer vision-based tracking systems utilize computer algorithms to process image frames captured by video cameras located in the construction site. Although numerous attempts have been made to address their deficiencies, computer vision-based tracking systems encounter issues such as abrupt movement, background clutter, scene illuminations, posture variations, scale variations, occlusions, and congestions (Konstantinou et al., 2019). On top of these challenges, computer vision-based tracking systems require a high number of cameras to have adequate coverage of the construction site and an extensive amount of data to train the algorithms, which further hinders their applicability in construction sites (Deng et al., 2021; Neuhausen et al., 2020). GPS, on the other hand, uses a trilateration technique to calculate a device's location, velocity, and elevation based on signals collected from satellites. Although GPS-based tracking systems do not require the installment of any additional devices on construction sites and can be employed using readily available GPS antennas in smartphones, they face significant challenges in terms of signal interference, which causes them to work improperly in densely populated urban settings and within buildings where signals can be attenuated by buildings (Sun et al., 2021). Although RFID systems emerge as a low-cost solution to locating the position of workers and materials indoors, the

challenges arising from their limited detection ranges and accuracy problems, especially when positioning moving objects, limit their widespread use (Xu et al., 2023). In contrast to all previously mentioned technologies, UWB technology stands as a promising alternative due to its high precision, high range, low latency, ability to stream real-time data, and ability to function in complex environments, such as inside of buildings (Mastrolembo Ventura et al., 2023).

While UWB technology has demonstrated significant potential, the accuracy and reliability of its implementation depend heavily on the placement of both tag and anchor sensors because of the NLOS condition that occurs when UWB signals are reflected or absorbed by objects such as furniture, equipment, and the human body (Yang et al., 2021). Despite the fact that the human body interferes with UWB signals, existing research has not comprehensively explored this aspect, leaving a gap in understanding the optimal configuration of tag sensors on the human body for worker tracking in construction environments. Thus, this study aims to evaluate the data collection performance of UWB sensors based on their placement on different parts of the body. By comparing different configurations, we aim to enhance construction safety through precisely monitoring construction workers in real time.

Methodology

For the evaluation of different tag placement locations on the human body, an experimental setup where participants walked on two perpendicular straight lines with moderate speeds was designed. All experiments were carried out in the Engineering Faculty building of Boğaziçi University, in a single environment, i.e., the corridor of the Civil Engineering department. Participants were asked to walk on two straight perpendicular lines with 240 cm and 390 cm lengths and completed 15 passes for each direction, totaling 30 passes for each axis and 60 passes per participant.

The UWB positioning system was developed using the commercially available UWB Transceiver Development Kit MDEK1001, which includes 12 DWM1001-DEV development boards, manufactured by QORVO. Four of the UWB sensors were deployed as anchor nodes and were placed on opposite walls of the building with a rectangular shape in the XY axis and were powered using 16340 3.7v lithium-ion rechargeable batteries with 850 mAh capacity. The anchor nodes are placed at different heights to improve trilateration accuracy. The distances between the anchors were measured using a laser meter, and the relative coordinates of each anchor were entered into the application provided by QORVO. The start and end points of both experiment routes were also measured using the same principle with a laser meter. Figure 1 shows a cross-section of the corridor, the positions of the anchors in XYZ, and the starting and ending points of two straight lines along which the participants were instructed to walk.

The UWB tags were placed on the different parts of each participant's body as pairs in a way that each pair's center point would coincide with the center point of the lines that participants walked over.

The placement of UWB tags was carefully determined based on practicality, relevance to real-life construction site environments, and expected tracking accuracy. One of our primary considerations was integrating UWB tags with standard construction safety gear, i.e., the hard hats and reflective safety vests. It is extremely easy to attach UWB tags to the hard hats using two-sided tapes, and most reflective safety vests have pockets at waist level, offering practical implementation potential without requiring additional effort. The head and waist also remain significantly more stable than moving limbs such as the feet or hands while walking, which is expected to improve tracking accuracy.

However, on top of practicality, the selection process also needed to consider how body interference affects UWB signals. For that, we first considered placing tags on the upper arms (below the shoulders) and on the upper thighs to analyze the impact of slight limb movement on tracking accuracy. However, the thigh placement was excluded and replaced with a below-the-knee placement due to discomfort caused by thigh muscle movement.

In the end, the selected body parts for each pair were around the head, attached to a hard hat (tags T1 and T2); around upper arms below the shoulders (tags T3 and T4); around the waist (tags T5 and T6); and below knee caps (tags T7 and T8). Figure 2 shows the placement of each sensor for one of the participants.

A total of 6 participants attended the experiments. Before the experiments, we measured the heights and weights of the participants. Additionally, we also recorded the heights of each tag relative to the floor before each experiment. Table 1 summarizes the height, weight, and relative tag height information for each participant.

Table 1: Height, Weight, and Tag Height Information for Each Participant

			Tag Heights Relative to Floor (cm)							
Participant ID	Height (cm)	Weight (kg)	T1	T2	T3	T4	T5	T6	T7	T8
1	189	95	182	182	134	134	109	109	47	47
2	163	53	160	160	120	120	100	100	41	41
3	180	80	181	181	140	140	119	119	51	51
4	188	105	181	181	135	135	113	113	47	47
5	180	80	184	184	139	139	122	122	56	56
6	194	98	186	186	142	142	112	112	51	51

There are two types of data collected during the experiment. The first one is the position of each tag in a relative XYZ coordinate system at a given time. This type of data was collected using a Python 3 code running on a Raspberry Pi 5, which was serially connected to a UWB tag configured as a listener. The data was collected and timestamped at 10 Hz, which is the maximum allowed

data recording rate of the devices. We started the data collection 15 seconds before and ended 15 seconds after each run. Figure 3 displays the data collection setup.

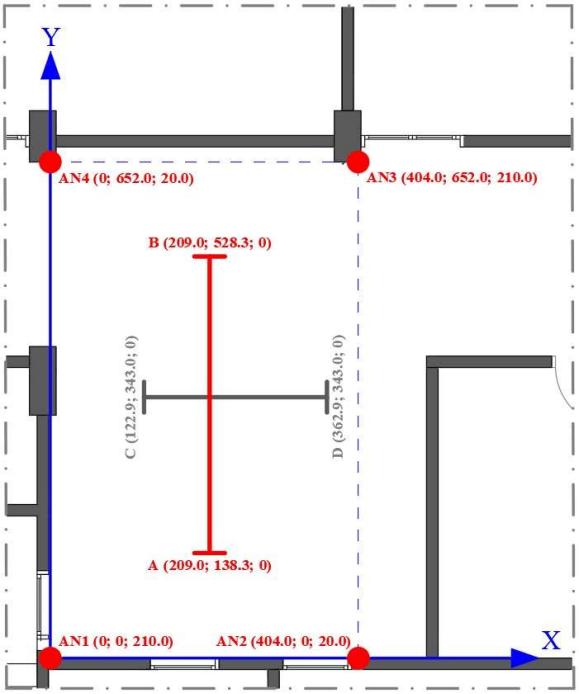

Figure 1: Experiment Environment, UWB Anchor Locations, and Experiment Routes

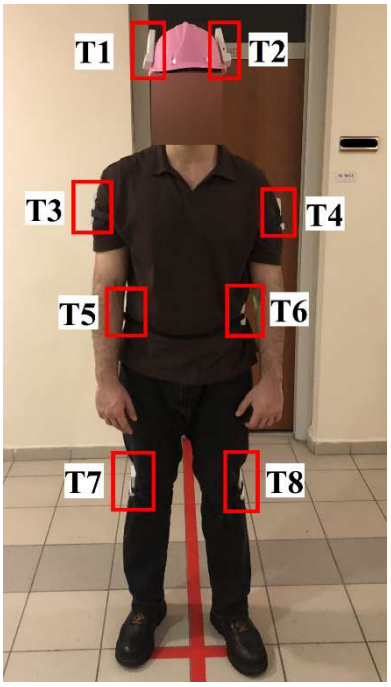

Figure 2: UWB Tag Placement and the Naming of Tags

The other type of data is the video recordings of each participant, which were recorded in 720p at 30 fps. The video recordings were later used to label the exact moments each participant was walking on the experiment route.

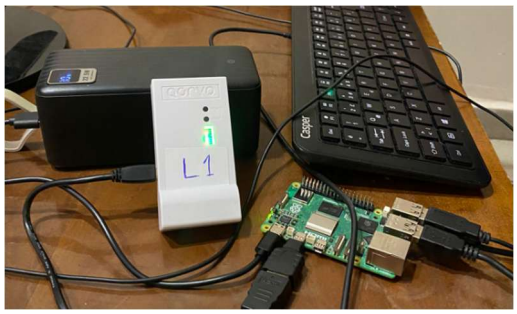

Figure 3: Raspberry Pi 5 - UWB Listener Tag Bundle Used for Data Collection

For data analysis purposes, the raw data was initially cleaned up using the labels that were created based on video footage. We analyzed each video frame by frame and used the exact start date and time of the videos to calculate the exact start and end Unix timestamp of each individual pass. We also calculated the average walking speeds of each participant by dividing the length of the experiment route by the average duration of their video clips. The data was then combined according to the previously mentioned pairs (i.e., body parts), and the locations of their centers and absolute error values were calculated for each data point.

The first thing we calculated was the amount of data collected for each tag and each tag pair. Theoretically, we should have gotten 10 data points per second. Using the start and end Unix timestamps of each run, we calculated the amount of data we should theoretically get and divided it by the amount of data we actually received during the experiments. We also calculated the amount of data received for each tag pair by considering the amount of data we received simultaneously for each pair, since we need to receive data from both of them at a given instance to calculate their center point.

Later, a single-sample two-sided t-Test was applied with a 95% confidence interval to evaluate whether the measured midpoints of each tag pair for each participant significantly differed from the theoretical line. Single-sample two-sided t-Test is a commonly used statistical test to determine whether the mean of a sample significantly differs or not from the population mean of a continuous variable (Walpole et al., 2012). In theory, the center of each tag pair should coincide with the coordinates of the experiment route. However, if we reject the null hypothesis based on the p-values, we can conclude that the center points do not coincide with the theoretical location of the experiment route.

Although t-Test requires normality for smaller sample sizes, this requirement can be omitted for larger sample sizes, such as the location data collected during the experiments. We assumed the distribution of the points had an unknown variance because the participants performed natural movements while walking. The proposed hypotheses for the T-test are as follows:

H_0: The measured center positions of the tag pair do not differ significantly from the expected location of the experiment route.

H_1: The measured center positions of the tag pair differ significantly from the theoretical location of the experiment route.

To compare the accuracy of measurements for different axes, an F-Test is applied to the absolute error values for each axis. The F-test is often used to see how different two sets of observations are from each other, like the data that an anchor setup records for different axes (Walpole et al., 2012). Firstly, we calculated the absolute error values for each tag pair. Next, we compared these values across different axes to determine the consistency of the sensor readings. The proposed hypotheses for the F-test are as follows:

H_0: There is not a significant difference between the variances of absolute error values of UWB tag pairs across the two experiment routes.

H_1: There is a significant difference between the variances of absolute error values of UWB tag pairs across the two experiment routes.

Lastly, the mean absolute error and the standard deviation of mean absolute error values are calculated for each tag pair and for each axis to compare the accuracy of alternative tag placements on the human body.

Results and Discussion

After careful examination of video footage and elimination of unsuitable runs due to the fall of loose tags and participant's loss of balance, we identified a total of 172 passes on the gray route and 180 passes on the red route to be appropriate for analysis. The experiments carried on the gray route took 391.2 seconds in total, whereas the ones carried on the red route took 567.7 seconds in total.

Participants completed the experiment route parallel to the X axis (gray route) in 2.067 seconds on average with an average speed of 4.18 km/h. On the other hand, it took 3.196 seconds on average to complete the experiment route parallel to the Y axis (red route), resulting in an average speed of 4.39 km/h. Table 2 summarizes the average walking speeds of each participant. The walking speeds of the participants during the experiments are relatively close to the preferred walking speed of humans, which is around 1.4 m/s (5.04 km/h) (Browning et. al, 2006).

Theoretically, 3912 data points should have been collected on the gray route, and 5677 data points should have been collected on the red route based on the durations of the experiments. However, a loss of signal occurs when the anchors cannot communicate with the UWB tags and is usually caused by interference with UWB signals resulting from body shadowing (due to both participants' own bodies and people occasionally using the corridor) and other objects in the experiment setting.

Thus, the actual number of data points collected differs from the theoretical value. Table 3 and Table 4 summarize the actual data point counts for different tags for experiments carried out on the gray route and red route. In addition, Table 5 and Table 6 summarize the actual data point counts for different tag pairs, i.e., the instances where the position of both tags of a pair are successfully measured, for the gray route and red route. The sensor pair placed on the head outperforms the other sensor pair placements by a great margin, achieving over 99% successful signal collection during the experiment carried out on both axes. On the other hand, the sensor pair located below the knees performed significantly worse, achieving below 30% successful signal collection. This is of particular importance especially when the goal is to track the worker positions uninterrupted in real-time. Tag pairs located below the shoulders, around the waist, and below the knees are fixed directly on the human body. However, the tag pair located on the head is fixed on a hard hat and not directly on the human body, resulting in approximately 3 centimeters of distance between the sensors and the human body. This might be the reason why there is a much lower amount of signal interference for the sensor pair located on the head compared to the other sensor pairs. Other sensor pairs also experience additional body shadowing due to the swinging of arms, while this is not the case for the sensor pair located on the head.

Another interesting finding is that the successful signal collection rates drop significantly across different axes for sensor pairs located on the shoulders and waist. For instance, the sensor pair located around the waist successfully collects a signal 75.92% of the time when the experiments are carried parallel to the X axis, but this value drops to 21.40% when the experiments are carried parallel to the Y axis. This might be the result of anchor configuration, since the anchors are located closer on the X axis.

Table 2: Walking Speeds of Each Participant on Different Experiment Routes

Participant ID	Average Time to Complete Gray Route (s)	Average Time to Complete Red Route (s)	Average Speed on Gray Route (km/h)	Average Speed on Red Route (km/h)
1	2.209	3.813	3.91	3.68
2	2.186	3.408	3.95	4.12
3	2.033	3.061	4.25	4.59
4	1.866	2.930	4.63	4.79
5	2.313	3.093	3.73	4.54
6	1.791	2.873	4.82	4.89

Table 3: Each UWB Tag's Actual and Theoretical Data Counts for Gray Route

Sensor Name	T1	T2	T3	T4	T5	T6	T7	T8
Actual Data Count	3888	3905	2932	3674	3365	3459	2390	2563
Theoretical Data Count	3912	3912	3912	3912	3912	3912	3912	3912
Data Received (%)	99.4%	99.8%	74.9%	93.9%	86.0%	88.4%	61.1%	65.5%

Table 4: Each UWB Tag's Actual and Theoretical Data Counts for Red Route

Sensor Name	T1	T2	T3	T4	T5	T6	T7	T8
Actual Data Count	5673	5664	3034	3755	2970	3756	2979	3476
Theoretical Data Count	5677	5677	5677	5677	5677	5677	5677	5677
Data Received (%)	99.9%	99.8%	53.4%	66.1%	52.3%	66.2%	52.5%	61.2%

Table 5: Actual and Theoretical Data Counts of Different Sensor Pairs for Gray Route

Sensor Pair	HEAD	SHOULDER	WAIST	KNEE
Actual Data Count	3881	2698	2970	1136
Theoretical Data Count	3912	3912	3912	3912
Data Received (%)	99.21%	68.97%	75.92%	29.04%

Table 6: Actual and Theoretical Data Counts of Different Sensor Pairs for Red Route

Sensor Pair	HEAD	SHOULDER	WAIST	KNEE
Actual Data Count	5660	1141	1215	875
Theoretical Data Count	5677	5677	5677	5677
Data Received (%)	99.70%	20.10%	21.40%	15.41%

Table 7 and Table 8 demonstrate the single-sample two-sided t-Test results. Test results indicate that the measured center points by tag pairs located at the shoulders, waist, and knees significantly differ from the theoretical line for both the gray route and red route. However, the test results fail to reject the H_0 for the tag pair located on the head for both the gray route and red route with a 95% confidence interval, meaning that the center points measured by the tag pair located on the head are not significantly different from the theoretical line. Based on the results, it can be concluded that the sensor pairs located below the shoulders, around the waist, and below the knees cannot be utilized to measure the center point of the path on which workers walk. However, the sensor pair located on the head might be used to locate workers' walking paths.

Table 9 shows the F-test results for different tag pairs. Based on the F-test results, the variances of the absolute error values differ significantly across different axes for all sensor pairs. In other words, the absolute error values exhibit different variances for the X and Y axes for every sensor pair. This indicates that none of the sensor pairs are capable of measuring a worker's location with consistent precision across both axes. For example, if we consider the sensor pair placed on the head, the test results demonstrate that this sensor pair cannot measure the worker's position with the same level of precision in the X-axis as it does in the Y-axis. This discrepancy in variance highlights a fundamental limitation in the ability of the sensors to provide equally reliable measurements across different spatial dimensions.

Table 7: Single Sample t-Test Results for Gray Route

Sensor Pair	HEAD	SHOULDER	WAIST	KNEE
Mean ($\bar{x}$)	3.42898	3.44225	3.44869	3.44296
Standard Deviation	0.07290	0.10897	0.07049	0.08696
Count (n)	3881	2699	2970	1136
Std. Error of Mean (SEM)	0.00117	0.00210	0.00129	0.00258
Degrees of Freedom (df)	3880	2698	2969	1135
Hypothesized Mean (μ)	3.43	3.43	3.43	3.43
t-Statistic	-0.87	5.84	14.45	5.02
Sig.	0.385	0.000	0.000	0.000

Table 8: Single Sample t-Test Results for Gray Route

Sensor Pair	HEAD	SHOULDER	WAIST	KNEE
Mean ($\bar{x}$)	2.08976	2.10507	2.12649	2.11855
Standard Deviation	0.10651	0.11233	0.10361	0.15307
Count (n)	5660	1141	1215	875
Std. Error of Mean (SEM)	0.00142	0.00333	0.00297	0.00517
Degrees of Freedom (df)	5659	1140	1214	874
Hypothesized Mean (μ)	2.09	2.09	2.09	2.09
t-Statistic	-0.17	4.53	12.28	5.52
Sig.	0.867	0.000	0.000	0.000

Table 9: F-test Results for Sensor Pairs Located at Different Parts of the Human Body

Sensor Pair	HEAD	SHOULDER	WAIST	KNEE
s_1^2	0.00204	0.00509	0.00202	0.00355
s_2^2	0.00377	0.00648	0.00644	0.01167
N_1	3881	2699	2970	1136
N_2	5660	1141	1215	875
F-Test	1.85	1.27	3.19	3.28
Sig.	0.000	0.000	0.000	0.000

Lastly, the mean absolute error and the standard deviation of absolute error values are calculated for different sensor pairs. Table 10 and Table 11 represent these values for different sensor placements for the gray route and red route.

For experiments carried out on the gray route, the sensor pair placed on the head has the lowest mean absolute error which is 5.722 centimeters. On the other hand, the sensor pair placed around the waist achieves the lowest standard deviation of absolute error, which is 4.490

centimeters. However, the standard deviation of absolute error for the sensor pair placed on the head is quite close to the lowest one at 4.517 centimeters. The sensor pair placed below the shoulders performs the worst both in terms of mean absolute error and standard deviation of absolute error.

For experiments carried out on the red route, the sensor pair placed around the waist has the lowest mean absolute error which is 7.504 centimeters. However, the sensor pair placed on the head achieves a significantly lower standard deviation of absolute error compared to the other sensor pair placements, with a standard deviation of absolute error of 6.142 centimeters. The sensor pair placed below the knees performs the worst both in terms of mean absolute error and standard deviation of absolute error during the experiments carried out on the red route.

The mean absolute error values are comparable to the findings of Dabove et al., 2018, but the standard deviations of absolute error values are comparatively higher. This difference in the standard deviation values might be explained by the nature of human walking during which the body tends to sway and the interference with UWB signals caused by the human body.

Table 10: Mean Absolute Error and Standard Deviation of Absolute Error Values of Different Sensor Pairs for Gray Route

Sensor Pair	HEAD	SHOULDER	WAIST	KNEE
Mean Absolute Error (m)	0.05722	0.08328	0.05747	0.06462
Standard Deviation of Absolute Error	0.04517	0.07134	0.04490	0.05962

Table 11: Mean Absolute Error and Standard Deviation of Absolute Error Values of Different Sensor Pairs for Red Route

Sensor Pair	HEAD	SHOULDER	WAIST	KNEE
Mean Absolute Error (m)	0.08702	0.07979	0.07504	0.11213
Standard Deviation of Absolute Error	0.06142	0.08048	0.08023	0.10804

Although the results indicate that head-mounted UWB tags provide the highest accuracy and highest data collection rate, practical considerations should also be taken into account. Construction workers frequently engage in tasks that require bending, crouching, or working at heights, which could affect the feasibility of helmet-mounted apparatuses. Worker comfort and compliance with safety regulations should be considered when recommending head-mounted UWB tracking systems. Considering the fact that helmets manufactured in Europe in compliance with EN 397 are typically between 300–500g in weight, and the tags that we used during the experiments weigh approximately 35 grams each (including the battery), the helmet-mounted tag apparatus can be designed to stay within the average weight range. (European Committee for Standardization, 2012). Future studies should investigate the long-term usability and acceptance of such sensor placements in actual construction workflows.

Conclusion

This study investigated the impact of different UWB tag placements on the human body on worker tracking accuracy in construction environments, focusing on four locations: around the head, around the upper arms (below the shoulders), around the waist, and below the knees. The test results showed that sensor placement in fact significantly affects the performance of UWB tags. The tag pair attached to the head achieved the highest accuracy and data collection success rate. Statistical analysis using a t-Test revealed that only the head-mounted sensor pair might accurately measure the theoretical walking path, as the center points of tags placed on around the shoulders, around the waist, and below the knees showed statistically significant deviations from the theoretical location of the experiment routes. These deviations are likely due to body shadowing effects, where UWB signals are blocked or absorbed by the human body, reducing tracking accuracy and successful signal collection. Additionally, the tag pair located on the head consistently achieved over 99% successful signal collection rates across both axes, significantly outperforming all other sensor placements in terms of successful signal collection.

However, despite the overall accuracy of UWB technology, F-test results indicated that no sensor pair maintains equal precision across both movement axes. The variance in absolute error values significantly differ across axes, suggesting that factors such as walking direction and anchor configuration contribute to measurement inconsistencies. For instance, the sensor pair located around the waist experienced substantial drop in performance when tracking movement along the Y axis, while performing significantly better on the X axis.

While these findings demonstrate the strong potential of UWB for real-time worker tracking, they also highlight certain limitations. The tests were conducted in a university corridor where individual participants moved along a predefined straight path, which does not fully replicate the dynamic and unstructured conditions of a construction site. While this setup ensures consistency in data collection, the controlled nature of the experiments does not fully capture the complexities of real-world construction sites, where body-to-body interference caused by other workers and construction machinery, and varying environmental conditions can affect tracking performance. Future research should aim to validate these findings in actual construction settings, where factors such as moving machinery, environmental interference, and interactions with other workers could

impact UWB tracking accuracy. Future experiments should incorporate multiple workers moving simultaneously to evaluate potential interference effects and better reflect practical applications. Additionally, while six participants provided sufficient data for statistical analysis, a larger sample size reflecting diverse body types and movement patterns would enhance the generalizability of the results.

To further optimization of UWB-based tracking for construction safety applications, future research should explore:

- More diverse and complex movement scenarios such as climbing stairs, crouching, or navigating obstacles and interaction with construction equipment and machinery to assess tracking accuracy of UWB tags under realistic work conditions.
- Loss of sight caused by body-to-body interference due to other workers operating in proximity.
- Alternative anchor configurations and use of additional anchors, particularly in dynamic environments, to minimize variance differences across X and Y axes.
- The integration of UWB with other sensing technologies, such as computer vision or wearable physiological sensors, to further enhance the robustness and applicability of real-time worker tracking solutions.

By addressing these challenges, future research can further refine UWB-based worker tracking, making it a more reliable and scalable solution for real-time safety monitoring and hazard prevention in construction environments.

References

Akinlolu, M., Haupt, T. C., Edwards, D. J., & Simpeh, F. (2020). A bibliometric review of the status and emerging research trends in Construction Safety Management Technologies. *International Journal of Construction Management*, *22*(14), 2699–2711. https://doi.org/10.1080/15623599.2020.1819584

Asadzadeh, A., Arashpour, M., Li, H., Ngo, T., Bab-Hadiashar, A., & Rashidi, A. (2020). Sensor-based safety management. *Automation in Construction*, *113*, 103128. https://doi.org/10.1016/j.autcon.2020.103128

Browning, R. C., Baker, E. A., Herron, J. A., & Kram, R. (2006). Effects of obesity and sex on the energetic cost and preferred speed of walking. *Journal of Applied Physiology*, *100*(2), 390–398. https://doi.org/10.1152/japplphysiol.00767.2005

Dabove, P., Di Pietra, V., Piras, M., Jabbar, A. A., & Kazim, S. A. (2018). Indoor positioning using ultra-wide band (UWB) technologies: Positioning accuracies and sensors' performances. *2018 IEEE/ION Position, Location and Navigation Symposium (PLANS)*, 175–184. https://doi.org/10.1109/plans.2018.8373379

Deng, H., Ou, Z., & Deng, Y. (2021). Multi-angle fusion-based safety status analysis of construction workers. *International Journal of Environmental Research and Public Health*, *18*(22), 11815. https://doi.org/10.3390/ijerph182211815

European Committee for Standardization. (2012). *EN 397:2012+A1:2012: Industrial safety helmets*. CEN

Eurostat. (2024, October). Accidents at work statistics: Number of accidents. https://ec.europa.eu/eurostat/statistics-explained/index.php?title=Accidents_at_work_statistics#Number_of_accidents

Konstantinou, E., Lasenby, J., & Brilakis, I. (2019). Adaptive Computer Vision-based 2D tracking of workers in complex environments. *Automation in Construction*, *103*, 168–184. https://doi.org/10.1016/j.autcon.2019.01.018

Mastrolembo Ventura, S., Bellagente, P., Rinaldi, S., Flammini, A., & Ciribini, A. L. (2023). Enhancing safety on construction sites: A UWB-based proximity warning system ensuring GDPR compliance to prevent collision hazards. *Sensors*, *23*(24), 9770. https://doi.org/10.3390/s23249770

Neuhausen, M., Herbers, P., & König, M. (2020). Using synthetic data to improve and evaluate the tracking performance of construction workers on site. *Applied Sciences*, *10*(14), 4948. https://doi.org/10.3390/app10144948

Newaz, M. T., Ershadi, M., Jefferies, M., Pillay, M., & Davis, P. (2022). A systematic review of Contemporary Safety Management Research: A multi-level approach to identifying trending domains in the construction industry. *Construction Management and Economics*, *41*(2), 97–115. https://doi.org/10.1080/01446193.2022.2124527

Soltanmohammadlou, N., Sadeghi, S., Hon, C. K. H., & Mokhtarpour-Khanghah, F. (2019). Real-time locating systems and safety in construction sites: A literature review. *Safety Science*, *117*, 229–242. https://doi.org/10.1016/j.ssci.2019.04.025

Sun, R., Wang, G., Cheng, Q., Fu, L., Chiang, K.-W., Hsu, L.-T., & Ochieng, W. Y. (2021). Improving GPS code phase positioning accuracy in urban environments using machine learning. *IEEE Internet of Things Journal*, *8*(8), 7065–7078. https://doi.org/10.1109/jiot.2020.3037074

Walpole, R. E., author, Myers, R. H., authorMyers, Sharon L. ,. authorYe, Keying, author, & Ronald E. Walpole, R. C., Ryamund H. Myers, Virginia Tech, Sharon L. Myers, Radford University, Keying Ye,

University of Texas at San Antonio. (2012). *Probability and statistics for engineers and scientists*. Pearson.

Xu, J., Li, Z., Zhang, K., Yang, J., Gao, N., Zhang, Z., & Meng, Z. (2023). The principle, methods and recent progress in RFID positioning techniques: A Review. *IEEE Journal of Radio Frequency Identification*, *7*, 50–63. https://doi.org/10.1109/jrfid.2022.3233855

Yang, X., Wang, J., Song, D., Feng, B., & Ye, H. (2021). A novel nlos error compensation method based IMU for UWB indoor positioning system. *IEEE Sensors Journal*, *21*(9), 11203–11212. https://doi.org/10.1109/jsen.2021.3061468